ELSEVIER

Thermochimica Acta 376 (2001) 51–61

thermochimica acta

www.elsevier.com/locate/tca

Thermal and morphological studies on ethylene-vinyl acetate copolymer–polyaniline blends

T. Jeevananda, Siddaramaiah*

Department of Polymer Science and Technology, S.J. College of Engineering, Mysore 570 006, India

Received 06 December 2000; received in revised form 02 April 2001; accepted 09 April 2001

Abstract

A series of ethylene-vinyl acetate copolymer–polyaniline (EVA–PAn) blends with different weight ratios of PAn were obtained by mechanical blending using plasticorder. Thermogravimetric analysis (TGA) studies of the blends were performed in order to establish the mode of their thermal degradation. The TGA thermograms showed that the thermal degradation of EVA–PAn blends was found to proceed in three steps except in the case of EVA–PAn (90/10) blend system. Degradation kinetic parameter was obtained for each stage of thermal degradation of blends, using Broido and Coats–Redfern methods. The activation energy (E) of the blends for the thermal degradation process lie in the range of 3.3–95.6 kJ/mol and of 9.6–135.0 kJ/mol for Broido and Coats–Redfern methods, respectively. The surface morphology of the EVA–PAn blends was analyzed by scanning electron microscopy (SEM) before and after thermal treatment.

Keywords: EVA; PAn; TGA; Thermal stability; Kinetic parameter

1. Introduction

Conducting polymers have attracted much attention from both fundamental as well as practical viewpoints. Among conducting polymers, polyaniline (PAn) is a promising candidate for its industrial importance due to its stability and potentially attractive economy. The disadvantages of PAn such as insolubility, infusibility, and hence non-processibility often hinder the potential applications. In order to overcome these disadvantages, attempts have been made to make blends/composites with conventional polymers, where the conducting PAn exists as the dispersed phase. On the other hand, ethylene-vinyl acetate (EVA) copolymer offers excellent ozone, weather resistance, and good mechanical properties. Several researchers [1–6] have studied the thermal stability of PAn both in the conducting and insulating forms by TGA and DTA. For knowing their processing behavior and to select the suitable material for given application, polymer technologist requires knowledge about their dimensional stability and thermal history. Knowledge of thermal stability and degradation behaviors is useful to modify the polymers for newer applications. The investigations on the thermal stability of conducting PAn and its blends are hence of great importance. Survey of the literature reveals that the thermal blending of EVA–PAn and its characterization such as physico-mechanical, electrical, and thermal degradation kinetics have not been studied.

* Corresponding author. Tel.: +91-821-512568; fax: +91-821-515770.
E-mail address: siddaramaiah@yahoo.com (Siddaramaiah).

0040-6031/01/$ – see front matter
PII: S0040-6031(01)00530-5

In the present study, conductive EVA–PAn blends have been analyzed for their thermal stability using thermogravimetric analysis (TGA) and surface morphology by scanning electron microscopy (SEM).

2. Experimental

Aniline (E. Merck, India) was distilled under nitrogen and stored at low temperature prior to use. Reagent grade ammonium persulfate, hydrochloric acid, *p*-toluene sulfonic acid (*p*-TSA), and sodium hydroxide (Sd Fine Chemicals, India) were used as received. EVA copolymer having density of 0.93 g/cm^3, MFI of 2 g per 10 min, vinyl acetate content of 12%, and softening point of 74°C were obtained from M/s Polyolefins Industries Ltd., India.

PAn was chemically synthesized by oxidation of aniline with ammonium persulfate in hydrochloric acid in large scale according to the procedure [7]. The PAn–HCl complex obtained was dedoped by stirring in 1% NaOH solution for 24 h and dried in a vacuum oven at 50°C for 24 h. The obtained dedoped PAn is referred as emeraldine base (EB). EB was mechanically mixed with *p*-TSA using an agate mortar and pestle for about 10–15 min with a weight ratio of 1:3 (EB:*p*-TSA). The weight average molecular weight (M_w) of the synthesized PAn lies in the range 43,500–45,750 g/mol.

A series of conductive blends of EVA and PAn/*p*-TSA complex were melt-blended in a Brabender plasticorder. The following sequence has been adopted to blend EVA with the conductive PAn. First, the temperature of the plasticorder was set to 150°C. After the temperature was attained, EVA was loaded and melt-mixed at 60 rpm for 5 min. Mechanically mixed PAn–TSA complex was then loaded with varying content (10–30%) to plasticorder with 40 rpm, and thoroughly blended with EVA for another 5 min. The obtained mass was made into sheets using compression molding at 150°C with a pressure of 3 tones for 1 min and cooled to room temperature by water circulation. Some of the typical properties of EVA, EVA–PAn blends, and PAn are given in Table 1.

The TGA thermograms were obtained using DuPont 2000 thermal analyzer at a heating rate of 10°C/min in air media. The TGA profiles were taken over a temperature range of 30–600°C. The weight of the sample used was 5 mg in all cases. Surface morphology of EVA–PAn blends was analyzed on JEOL (JSM-840A) SEM at an accelerating voltage of 10 kV. The samples were gold-sputtered prior to SEM observation.

The integral procedural decomposition temperature (IPDT) is defined as a means of summing up the whole shape of the normalized data curve. IPDT as an index of thermal stability was determined from the thermogram area using the method reported in the literature [8]. The oxidation index (OI) was calculated based upon the weight of carbonaceous char (CR) as related by the empirical equation

$$\mathrm{OI} \times 100 = 17.5 \times 0.4\mathrm{CR} \quad (1)$$

The thermal degradation kinetic parameters for EVA, EVA–PAn blends, and PAn were measured from the TGA thermogram using Broido [9] and Coats–Redfern [10] methods which provide overall kinetic data averaged for the experimental temperature range. For the sake of the calculations and to know the nature of the decomposition, the complete thermogram was

Table 1
Typical properties of EVA, EVA–PAn blends, and PAn

Blend composition EVA–PAn (%, w/w)	Density (g/cm^3)	Tensile strength ± 2 (MPa)	% Elongation at break ± 3	Conductivity ± 4 (S/cm)
100/0 (pure EVA)	0.930	22.1	445	2.27×10^{-15}
90/10	1.018	9.0	182	5.37×10^{-11}
85/15	1.051	6.7	103	3.00×10^{-10}
80/20	1.103	5.4	41	6.00×10^{-9}
75/25	1.111	4.5	22	1.20×10^{-8}
70/30	1.160	4.1	18	4.37×10^{-8}
0/100 (pure PAn)	1.220	–	–	2×10^{-1}

divided into three distinct sections. The activation energy (E) for the thermal degradation processes was evaluated using Broido equation:

$$\ln\left[\ln\frac{1}{y}\right] = -\frac{E}{R}\left(\frac{1}{T} + K\right) \quad (2)$$

where R is the gas constant, T the temperature (in K), K any constant, y the normalized weight (w_t/w_0), and E the energy of activation can be obtained form the plot of $\ln[\ln(1/y)]$ verses $1/T$.

Coats–Redfern equation is as follows:

$$\log\left[\frac{-\ln(1-\alpha)}{T^2}\right] = \log\frac{ZR}{\beta E}\left(1 - \frac{2RT}{E}\right) - \frac{E}{2.303RT} \quad (3)$$

where α is the fraction of sample decomposed at T, Z the frequency factor, β the heating rate, and E the activation energy. A plot of $\log[-\ln(1-\alpha)/T^2]$ versus $1/T$ gives the slope for evaluation of the activation energy (E) most appropriately.

3. Results and discussion

3.1. Thermal analysis

TGA and its derivative thermograms for EVA and PAn homopolymers are given in Fig. 1(a) and (b), respectively. Typical TGA thermogram for all EVA–PAn blends are shown in Fig. 2. Fig. 1(a) shows two-step weight loss for EVA in the temperature ranges 300–410 and 410–520°C. The first-step weight loss is due to degradation of vinyl acetate group of EVA which looses acetic acid at higher temperature and the second-step weight loss can be attributed to the degradation of main ethylene chain [11]. The TGA thermogram of PAn (Fig. 1(b)) shows three-step weight loss process, which is similar to the observation done by Chan et al. [4]. The first step occurs in the range 65–125°C which is attributed to the expulsion of water molecule from the polymer matrix. The second-step weight loss occurs between 125 and 350°C which is due to the loss of low molecular weight polymer and unbounded dopant p-TSA from PAn chain. The third-step weight loss occurs between 350 and 520°C which is due to the degradation of main chain PAn after elimination of bounded dopant.

The TGA thermograms of all EVA–PAn blends shows three significant thermal degradation steps (Fig. 2) at 250, 445, and 495°C (Table 2) for first-, second-, and third-step weight losses, respectively, except in the case of EVA–PAn (90/10) blend system. Two-step weight loss in the case of EVA–PAn (90/10) blend may be due to lower content of PAn in EVA matrix and is completely embedded in continuous EVA matrix. In the case of other combinations, the first-step weight loss can be attributed to the loss of loosely bounded water, excess unbounded and partly bounded dopant which occurs in the temperature range 65–405°C. Although, the co-evolution of other species such as oxidant, oligomers, and vinyl acetyl group of EVA were not ruled out with a weight loss of 34.0–43.3%. The second-step weight loss occurs in the temperature range 420–465°C which represents the loss of remaining bounded dopant (p-TSA) in PAn with a weight loss of 10.7–26.6%. The last and final-step weight loss occurs in the temperature range 465–525°C, indicating the complete decomposition of the skeletal of both polymer chain structures with a weight loss of 20.6–33.4%.

The temperature range of decomposition, the percentage weight loss, and the percent of ash are given in Table 2 for EVA, EVA–PAn blends, and PAn. From Table 2, it can be seen that increase in the PAn content increases the weight loss in the first step. This is due to the fact that increase in PAn content increases the moisture content and excess dopant (p-TSA) in the EVA–PAn blends. It can also be observed from Table 2 that the pure EVA and PAn show low ash content, whereas their blends show higher ash content. The higher ash content of the blends can be explained on the basis that the intermediate pyrolyzed product (carbonized residue) formed during degradation of PAn may act as a radical scavenger for EVA degradation.

The thermograms obtained during TGA scans were analyzed to give the percentage weight loss as a function of temperature. T_0 (temperature of onset decomposition), T_{10} (temperature for 10% weight loss), and T_{max} (temperature for maximum weight loss) are the main criteria to indicate the thermal stability of the blends. Higher the values of T_0, T_{10}, T_{20}, and T_{max}, higher the thermal stability. The relative thermal stability of EVA–PAn blends were evaluated by comparing decomposition temperatures at various

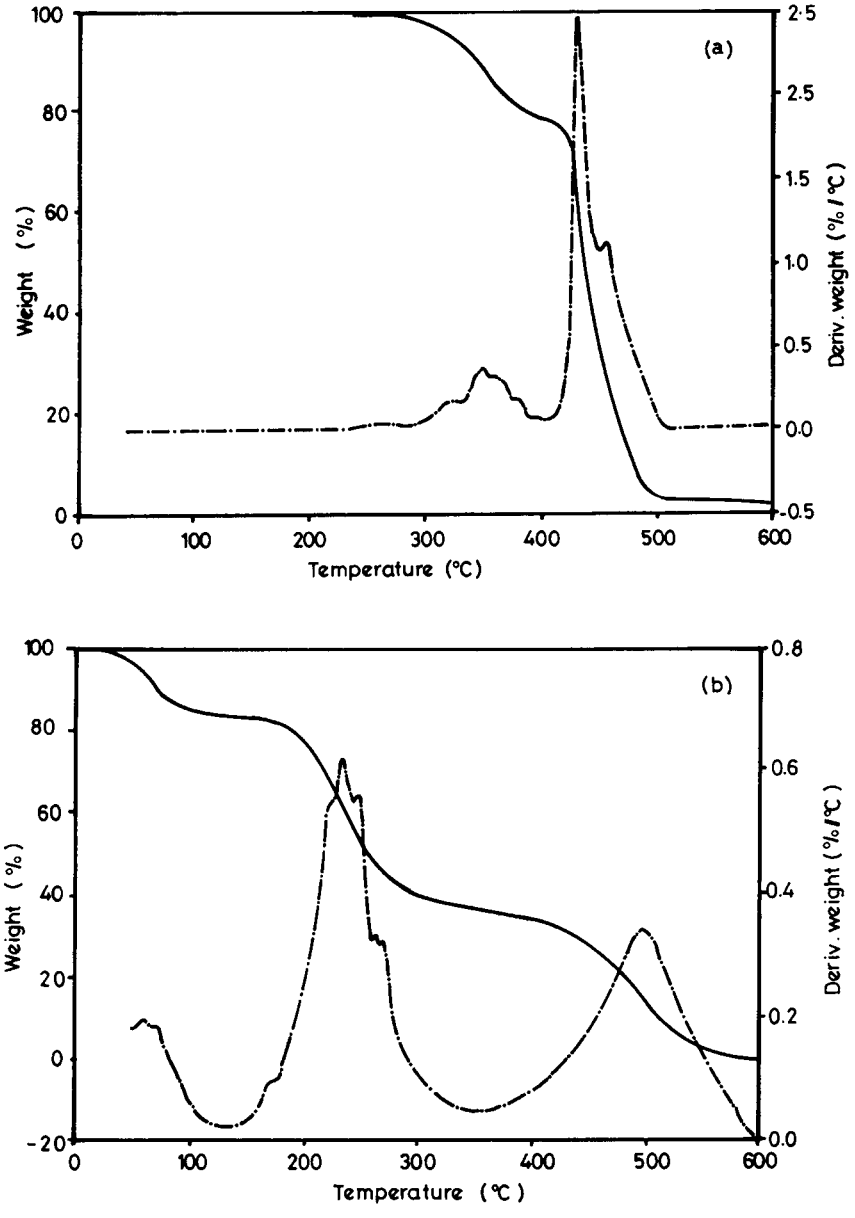

Fig. 1. TGA and its derivative thermograms of (a) EVA and (b) PAn homopolymers.

percentage weight losses and IPDT values given in Table 3. IPDT value represents the overall nature of the thermogram over the entire range of the TGA curves. From Table 3, it can be seen that the thermal stability of PAn is improved after blending with EVA matrix. IPDT value decreases with increase in PAn content. That means, 10% PAn-filled EVA system shows higher value compared to other blends because of its homogeneous morphology. This result clearly indicates two phase morphology of the blends except for 10% PAn-filled system. The IPDT values of all blends lie between IPDT values of individual components and lesser than corresponding additive values. Based upon the mass of carbonaceous char, it is

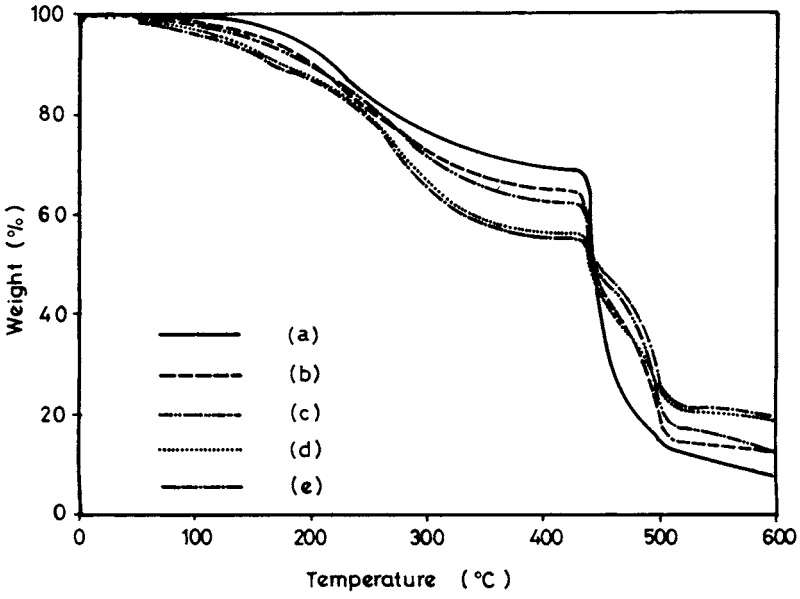

Fig. 2. TGA thermograms of EVA–PAn blends: (a) 90/10; (b) 85/15; (c) 80/20; (d) 75/25; (e) 70/30.

concluded that EVA–PAn blends are not good flame-retardant as evident by their OI values. It can also be seen from Table 3 that the OI values are almost same for all blends and lie in the range 0.602–1.351.

Kinetic parameters were evaluated from the TGA curves using Broido and Coats–Redfern method. The plots of $\ln[\ln(1/y)]$ and $\log[-\ln(1-\alpha)/T^2]$ verses $1/T$ for second and third stages of the thermal degradation processes of the blends are shown in Figs. 3(a) and (b), and 4(a) and (b) for Broido and Coats–Redfern methods, respectively. Regression analysis was carried out for both plots. The mechanism having R^2 close to unity was chosen. The regression analysis gives the results of slopes, constants, and R^2 values corresponding to each step of thermal degradation. The R^2 and calculated activation energy (E) for each step thermal degradation process are tabulated in Tables 4 and 5 for Broido and Coats–Redfern methods, respectively. The lowest E values were observed for the first-step thermal degradation compared to other two steps for both methods. This is due to lower energy required to remove loosely bounded water and excess dopant in the blends. Higher E values were observed for second and third steps, because higher energies are required for bond scission and unzipping of polymer chains.

3.2. Surface morphology

The polymer blend properties are strongly influenced by the morphology of the system. The SEM micrographs of pure EVA, EVA–PAn (90/10), and EVA–PAn (80/20) are shown in Fig. 5(a–c), respectively. In case of blends, the minor phase (PAn) is dispersed in the major continuous EVA phase. The EVA–PAn (90/10) blend system shows homogeneous morphology because of uniform distribution of PAn in EVA matrix (Fig. 5(b)). It can be seen from Fig. 5(c) that above 20% PAn addition to EVA matrix, the domain size of PAn increases/phase separation occurs due to aggregation of PAn in EVA matrix.

The effect of thermal treatment on surface morphology of the blends has been studied. The samples were subjected to heat treatment at 200, 300, and 400°C for 1 h. After thermal treatment, the surface morphology of the above samples were recorded by SEM. There was no significant change in the surface morphology of samples treated at 200°C. A maximum weight loss of 60% occurred and charred powder was obtained for the samples treated at 400°C. So, we have not recorded SEM for these samples. The samples treated at 300°C have shown significant change in

Table 2
Data obtained from TGA analysis of EVA, EVA–PAn blends, and PAn

Blend composition EVA–PAn (%, w/w)	Process	Transition range (°C)[a]			Weight loss (%)
		T_i	T_d	T_c	
100/0 (pure EVA)	1	300	350	410	21.33
	2	410	440	520	75.33
	Ash	–	–	–	3.33
90/10	1	120	220	400	29.3
	2	400	450	530	62.0
	Ash	–	–	–	8.6
85/15	1	100	250	410	34.0
	2	410	445	465	26.6
	3	465	495	525	28.7
	Ash	–	–	–	10.6
80/20	1	80	280	420	36.0
	2	420	445	460	18.0
	3	460	490	525	33.4
	Ash	–	–	–	12.6
75/25	1	70	280	405	42.6
	2	405	445	465	17.4
	3	465	495	525	20.6
	Ash	–	–	–	19.3
70/30	1	65	280	415	43.3
	2	415	445	460	10.7
	3	460	495	525	27.3
	Ash	–	–	–	18.6
0/100 (pure PAn)	1	65	75	125	15.8
	2	125	245	350	49.2
	3	350	500	520	33.0
	Ash	–	–	–	2.0

[a] T_i: temperature at which decomposition starts; T_d: temperature at which decomposition rate is maximum; T_c: temperature at which decomposition is completed.

Table 3
Data obtained from TGA analysis of EVA, EVA–PAn blends, and PAn

Blend composition EVA–PAn (%, w/w)	Temperature at different weight loss[a] ± 2 (°C)					IPDT ± 2	OI ± 2
	T_0	T_{10}	T_{20}	T_{50}	T_{max}		
100/0 (pure EVA)	250	350	380	440	500	814	0.2331
90/10	100	225	280	450	530	766	0.6020
85/15	95	210	270	450	525	671	0.7420
80/20	80	205	265	445	525	699	0.8820
75/25	70	180	255	445	525	584	1.3510
70/30	68	180	250	440	525	594	1.3020
0/100 (pure PAn)	65	75	180	255	520	540	0.1400

[a] T_0: temperature of onset decomposition; T_{10}: temperature of 10% weight loss; T_{20}: temperature of 20% weight loss; T_{50}: temperature of 50% weight loss; T_{max}: temperature at which decomposition is completed.

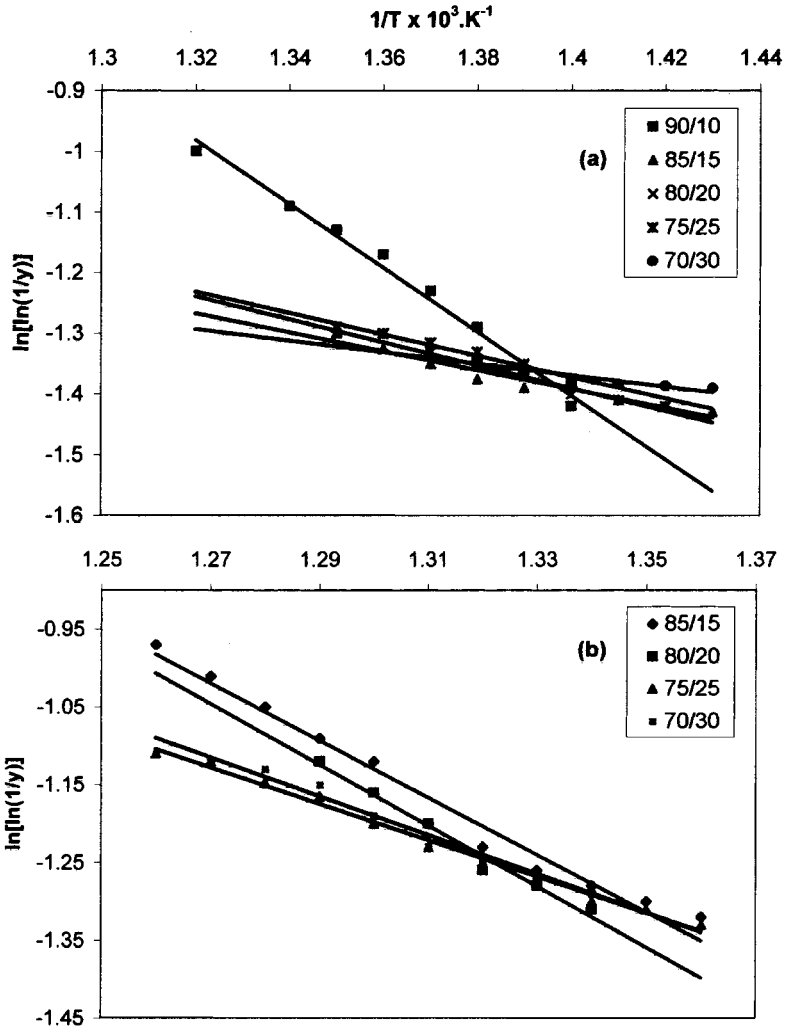

Fig. 3. Typical Broido plot for the determination of activation energies for (a) second-step and (b) third-step weight loss of EVA–PAn blends.

Table 4
Broido treatment of kinetic parameters for the thermal degradation of EVA, EVA–PAn, and PAn systems

Blend composition EVA–PAn (%, w/w)	First step		Second step		Third step	
	$E \pm 2$ (kJ/mol)	R^2	$E \pm 2$ (kJ/mol)	R^2	$E \pm 2$ (kJ/mol)	R^2
100/0 (pure EVA)	18.8	0.9752	91.7	0.9877	–	–
90/10	6.5	0.9777	95.6	0.9886	–	–
85/15	3.3	0.9583	29.6	0.9439	70.4	0.9755
80/20	4.1	0.9844	36.0	0.9723	74.8	0.9828
75/25	4.2	0.9237	33.5	0.9670	45.0	0.9923
70/30	4.5	0.9437	18.0	0.8393	47.8	0.9760
0/100 (pure PAn)	1.6	0.9151	13.5	0.9671	36.2	0.9439

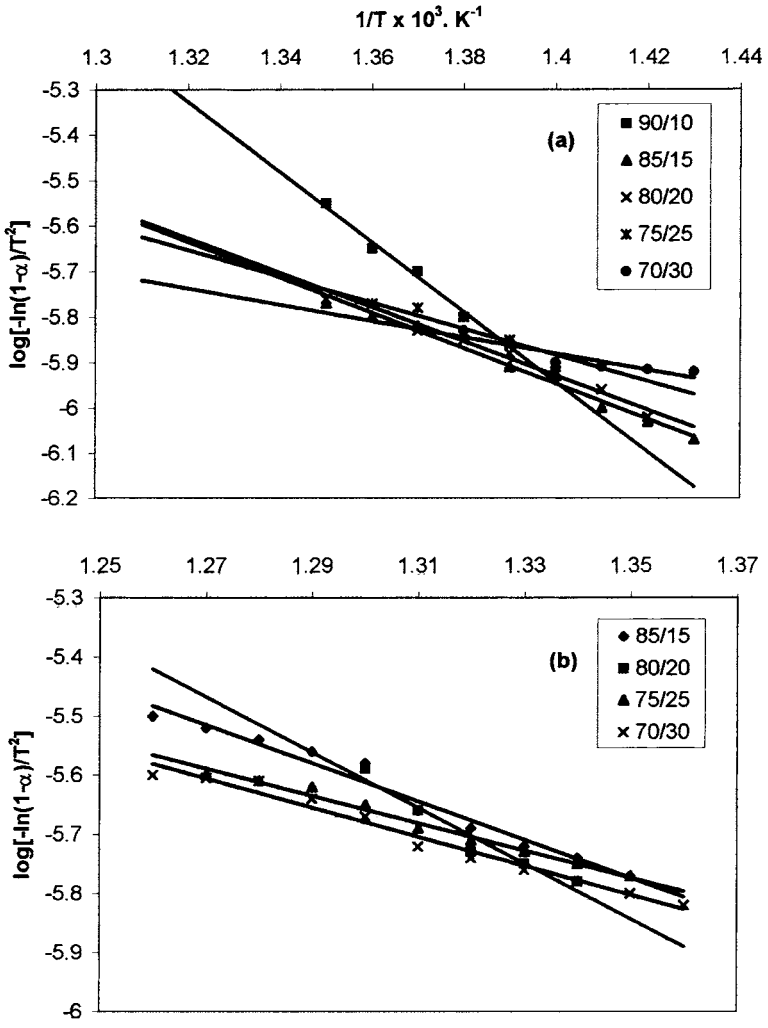

Fig. 4. Typical Coats–Redfern plot for the determination of activation energies for (a) second-step and (b) third-step weight loss of EVA–PAn blends.

Table 5
Coats–Redfern treatment of kinetic parameters for the thermal degradation of EVA, EVA–PAn, and PAn systems

Blend composition EVA–PAn (%, w/w)	First step		Second step		Third step	
	$E \pm 2$ (kJ/mol)	R^2	$E \pm 2$ (kJ/mol)	R^2	$E \pm 2$ (kJ/mol)	R^2
100/0 (pure EVA)	79.5	0.9339	92.1	0.9330	–	–
90/10	14.4	0.7835	135.0	0.9901	–	–
85/15	9.6	0.9856	74.5	0.9797	60.8	0.9735
80/20	10.3	0.9699	66.1	0.9723	61.8	0.9408
75/25	12.6	0.9721	55.1	0.8735	42.9	0.9830
70/30	11.7	0.9920	35.1	0.8558	43.9	0.9769
0/100 (pure PAn)	5.1	0.7131	19.4	0.9700	23.9	0.7893

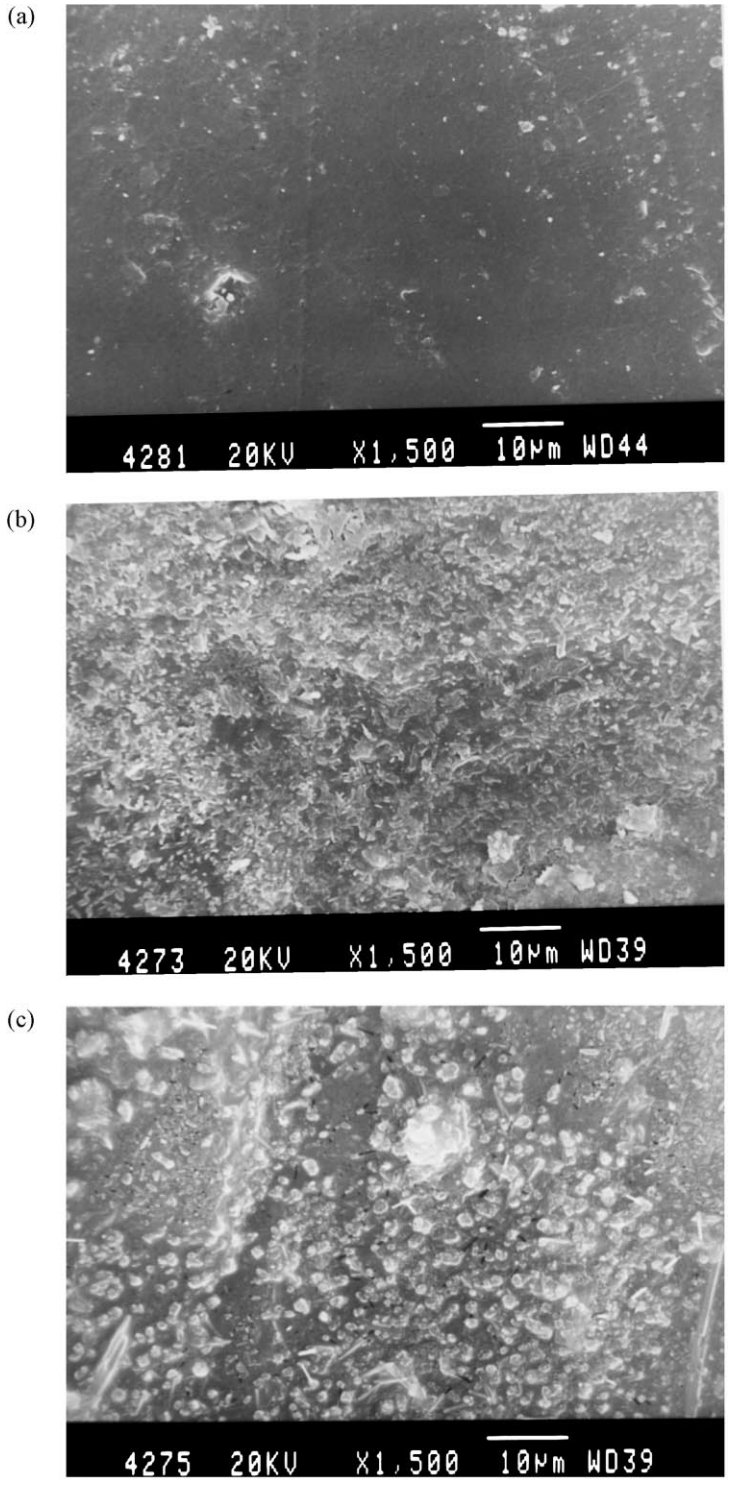

Fig. 5. SEM micrographs of (a) pure EVA, (b) EVA–PAn (90/10), and (c) EVA–PAn (80/20) blends.

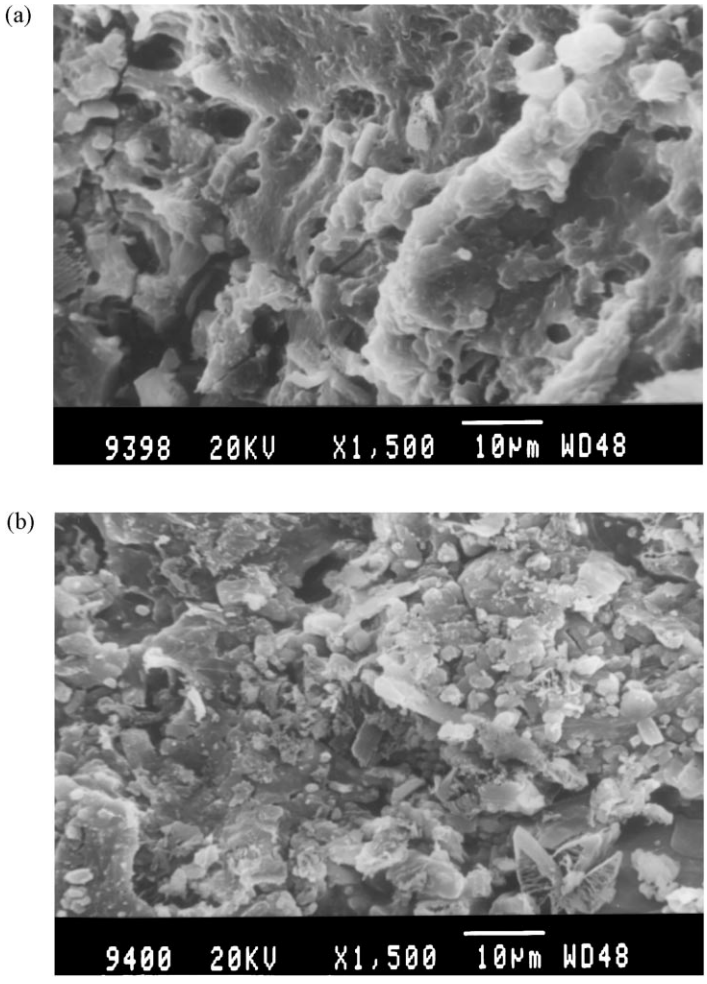

Fig. 6. SEM micrographs of (a) EVA–PAn (90/10) and (b) EVA–PAn (80/20) blends thermally treated at 300°C for 1 h.

morphology. The SEM micrographs of thermally treated (at 300°C for 1 h) EVA–PAn (90/10) and EVA–PAn (80/20) blends are shown in Fig. 6(a) and (b), respectively, which clearly indicates the formation of microvoids on the surface of the EVA matrix. These voids are due to the loss of volatile content and excess unbounded dopant from the EVA surface.

4. Conclusions

The following conclusions can be drawn from the present investigation.

1. The thermal stability of PAn is improved after blending with EVA matrix.
2. TGA curves show three significant thermal degradation steps at 280, 445, and 490°C for all EVA–PAn blends, except in the case of EVA–PAn (90/10) system.
3. Lowest activation energy (E) was observed for the first-step thermal degradation compared to second and third step, this is because less energy is utilized to remove the loosely bounded water and excess dopant.
4. The surface morphology reveals that the domain size is increased with increase in PAn content and the phase separation occurs due to saturation of

PAn in EVA matrix. Microvoids were observed on the surface of the EVA–PAn blends after thermal treatment.

Acknowledgements

One of the authors (Mr. T. Jeevananda) thanks the CSIR, New Delhi, India, for SRF fellowship (8/452 (1)/2000 – EMR-I-SPS).

References

[1] M.C. Gupta, S.S. Umare, Macromolecules 25 (1992) 138.
[2] S.H. Khor, K.G. Neoh, E.T. Kang, J. Appl. Polym. Sci. 40 (1990) 2015.
[3] V.G. Kulkarni, L.D. Campbell, W.R. Mathew, Synth. Met. 30 (1989) 321.
[4] H.S.O. Chan, P.K.H. Ho, E. Khor, M.M. Tan, K.L. Tan, B.T.G. Tan, Y.K. Lim, Synth. Met. 31 (1989) 95.
[5] L. Ding, X. Wang, R.V. Grogory, Synth. Met. 104 (1999) 73.
[6] N. Chandrakanthi, M.A. Careem, Polym. Bull. 44 (2000) 101.
[7] A.G. Mac Diarmid, J.C. Chiang, A.F. Epstein, Synth. Met. 18 (1987) 285.
[8] C.D. Doyle, Anal. Chem. 33 (1961) 77.
[9] A. Broido, J. Polym. Sci. Part A-2 7 (1969) 1761.
[10] A.W. Coats, J.P. Redfern, Nature 68 (1964) 201.
[11] R.B. Seymour, C.E. Carraher Jr., Structure–Property Relationship in Polymers, Plenum Press, New York, 1984.